EVALUATION OF RE-ENTRY CONDITIONS FROM ORBITS AT THE LIBRATION POINTS

F. Letizia[(1)], J. Siminski[(2)], S. Lemmens[(2)], and F. Renk[(2)]

[(1)] *University of Southampton, SO17 1BJ Southampton, United Kingdom, Email: f.letizia@soton.ac.uk*
[(2)] *European Space Agency, 64293 Darmstadt, Germany, E-mail: {Jan.Siminksi, Stijn.Lemmens, Florian.Renk}@esa.int*

ABSTRACT

Even if no protected regions are currently defined around the Sun-Earth libration points, missions in these orbits still have to be compliant with Space Debris Mitigation guidelines, for example for what concerns the casualty risk in case of re-entry. Past studies on the re-entries from libration orbits were carried out by performing a limited sensitivity analysis of the casualty area to the variation of re-entry parameters. In the current work, a Monte Carlo approach is used to study the evolution of trajectories in case of a fragmentation or a failure of a spacecraft at the libration points. A large number of possible re-entry trajectories are generated and the corresponding re-entry conditions and casualty area are obtained by simulating the last phase of the evolution with ESA DRAMA software. The goal is to find a practical procedure for casualty risk requirements verification for current and future missions.

Key words: re-entry; Monte Carlo; libration points.

1. INTRODUCTION

In these years we are observing an increase in the number of mission located at the Sun-Earth libration (SEL) points and the trend seems to hold for the future with the plans for missions such as Plato, Euclid, Athena, and the James Webb Space Telescope. Whereas no protected regions are defined for orbits at the libration points, the compliance of these missions with constraints coming from Space Debris Mitigation guidelines still needs to be checked, for example for what concerns the casualty risk in case of re-entry.

Several studies have considered the possibility of a re-entry from Libration Points Orbits (LPO), mainly as a possible disposal option [3, 10]. For example, Alessi [1] studied in detail the trajectory evolution from SEL points to Earth re-entry, analysing how re-entry represents a viable disposal option also for this class of missions. Alessi [1] also provides an analysis of the re-entry conditions (e.g. flight path angle, entry velocity) that can be used as a first proxy for the risk posed by a re-entry. In order to obtain a quantitative evaluation of the casualty risk associated to this kind of re-entries, past studies were carried out by performing a limited sensitivity analysis of the casualty area to the variation of re-entry parameters such as the flight path angle and the latitude at the re-entry in the atmosphere, measured at a reference altitude (e.g. 120 km). This was combined with worst case break-up assumptions and it is based on the hypothesis that an object from the libration points can reach the Earth at any latitude and longitude.

This last assumption derives from the study by Landgraf and Jehn [6] who analysed the consequences of a fragmentation at a SEL points, stating that objects generated by such a breakup "*can impact the Earth at any latitude, because the Earths diameter small is compared to the distance* [between the Earth and the SEL point]". For this reason, casualty risk analysis for re-entry trajectories from LPO are usually performed assuming a uniform distribution for this angle.

A different approach is proposed in the current work. Two scenarios are considered. First, a simple fragmentation on a LPO is studied to replicate the analysis by Landgraf and Jehn [6]. Secondly, given the operational orbit of a spacecraft, it is assumed that a failure can occur at any epoch. The state at the failure epoch is used to generate the initial condition for the trajectory propagation. For both scenarios, the propagation is performed taking into account the gravitational effect of main celestial bodies, the effect of the oblateness of the Earth, and solar radiation pressure. For the trajectories that re-enter in the atmosphere, the re-entry conditions (namely the velocity, the flight path angle and the latitude) are computed. In this way, a distribution of these parameters is obtained and their correlation can be evaluated.

Finally, the conditions at the atmosphere interface obtained with this approach can be set as initial conditions for tools specifically developed to study the re-entry phase. In the current application, ESA DRAMA was used for the computation of the resulting casualty area for each condition. In this way, the compliance of a mission to requirements can be assessed. The same workflow can be used to study different phase of a mission, as, for example, the disposal.

2. SNAPPSHOT

For this analysis, the tool SNAPPshot was used. SNAPPshot was initially developed to study the compliance of ESA missions with planetary protection requirements by using a Monte Carlo approach [8]. For this purpose, SNAPPshot is composed by three main modules. The first one sets the Monte Carlo simulation by determining the required number of runs and generating the corresponding initial conditions. The second block is a propagator that describes the evolution of the trajectories under the gravitational effect of the main bodies in the solar system and under the solar radiation pressure. The third module is the representation of the trajectories on the b-plane of the Earth or of other planets to detect conditions of impact or resonance.

The same structure can be kept also for the study of the compliance with Space Debris mitigation guidelines and some general improvements to the tool were introduced. Firstly, the re-entry analysis requires knowing the object status at a specific altitude, which represents the interface with the atmosphere. The status at the interface (set at 120 km of altitude) can then be used as initial condition for the propagation of the last leg of the trajectory with specific tools such as DRAMA [2]. To generate these states at the interface in an efficient way, the capability of event location of SNAPPshot propagator was enhanced by adopting an algorithm based on the *regula falsi* to obtain the object status at a certain altitude with the same level of accuracy used for the trajectory propagation.

The results in this work were obtained, as in the previous ones [8, 9], carrying out the trajectory propagation with respect to the Solar System Barycentre, but now SNAPPshot has the capability of specifying a different centre of integration. This option may be useful for future developments of the tool beyond the initial application to planetary protection. In any case, the object status at the atmosphere boundary is translated into a state in the Earth centred inertial frame and this format is used for the interface with DRAMA. Relevant quantities for the re-entry characterisation (e.g. velocity, flight path angle, latitude) are generated also by SNAPPshot directly starting from the state vector at the atmosphere boundary. In this case, the values (e.g. altitude and latitude) refer to the Earth considered as a sphere.

SNAPPshot force model was also updated by adding the contribution from the J_2 effect of the Earth. This was done because trajectories studied in this work, differently from the ones in [8, 9], may cross multiple times the Low-Earth Orbit (LEO) region. In any case, it was observed that the impact of J_2 on the distribution of the re-entry parameters is only marginal given the flight path angles involved when reaching the atmospheric interface. Finally, the possibility of providing the evolution of the trajectories also on rotating frames was added.

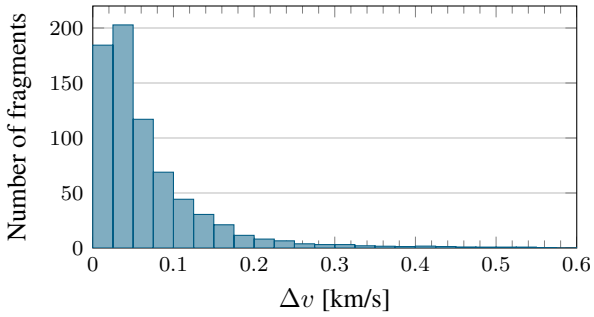

Figure 1. Distribution of the Δv among the fragments. Twenty runs of the breakup model were executed and the average values are shown.

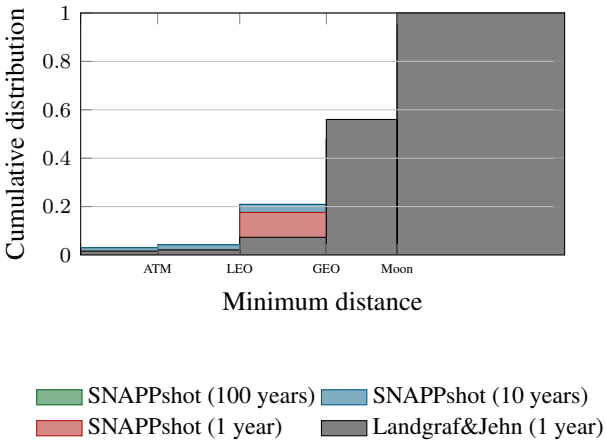

Figure 2. Cumulative distribution of the minimum distance from the Earth over different propagation time spans.

3. FRAGMENTATIONS ON ORBITS AT THE LIBRATION POINTS

To replicate the study by Landgraf and Jehn [6] on the analysis of a fragmentation at one of the SEL points, an explosion was considered. Differently from [6], NASA breakup model [4] was used to generate the debris cloud. Twenty runs of the model were performed to give statistical meaning to the results. The generated debris cloud is formed by 718 fragments larger than 5 cm and the distribution of the ΔV among the fragments is shown in Fig. 1. The distribution appears qualitatively similar to the one in [6] as in both cases one can observe a peak around 50 m/s and maximum value larger than 400 m/s. The area-to-mass ratio of the fragments is also obtained from the breakup model, with values ranging between 0.0017 and 22 m^2/kg. First, the case of an explosion at L_1 is considered.

The trajectory of each fragment was propagated for a maximum of 100 years and the minimum distance from

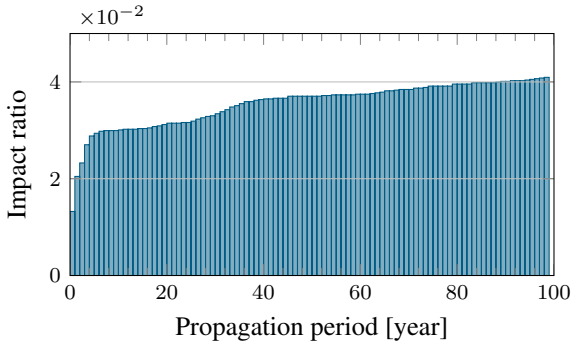

Figure 3. Variation of the impact ratio with the propagation time.

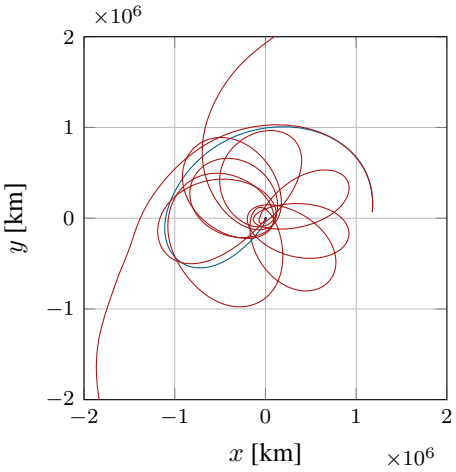

Figure 4. Two impact trajectories represented in a rotating reference frame with the Earth in the centre and the Sun in the positive side of the x-axis.

the Earth checked. Fig. 2 shows the distribution of the minimum distance; the four thresholds in the x-axis refers to 1) objects that go below 120 km of altitude (ATM), 2) below 2000 km (LEO), 3) below the GEO (Geostationary Earth Orbit) altitude, and, finally, below the Earth-Moon distance. The percentage of fragments that impact the Earth and that cross the LEO region are consistent with the results in [6] where these values are respectively 1.6% and 2.1%, whereas the SNAPPshot provides (for one year of propagation) 1.3% and 1.9%. The percentage of fragments that go below the Earth-Moon distance is slightly difference in the two models, but it should be pointed out that Landgraf and Jehn [6] do not provide this value in this work, but rather the one of the in-bound trajectories and not all of them actually have a perigee smaller than the lunar distance.

As the propagation time is increased, a larger share of fragments reaches the Earth. Fig. 3 shows the evolution of the ratio of impacts over the total number of trajectories. One can observe a clear change in the rate of variation of this parameter around 35-40 years (and then, in a less pronounced way, around 65 years).

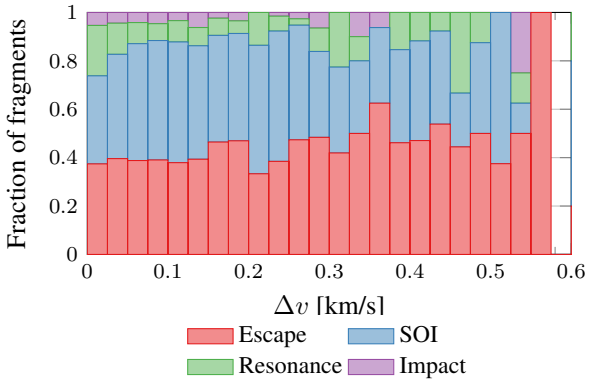

Figure 5. Distribution of the trajectory status with the Δv due to the breakup. SOI indicates close approaches within the sphere of influence of the Earth.

These trajectories with late re-entry can be characterised by multiple passages in the *proximity* of the Earth as shown in Fig. 4. For this visualisation, the same rotating frame as in [6] was used: the origin of the system is in the centre of the Earth, whereas the Sun is located on the x-axis, on the positive side. The first trajectory (in blue) represent a *direct* re-entry that occurs in less than four months (108 days). In the second case (in red) the object impacts the Earth after 59 years and nine close approaches.

As explained in detail in [8], SNAPPshot does not register only impacts but also conditions of resonance with a planet and entrance in its sphere of influence (SOI). Fig. 5 shows the correlation between the trajectory *category* and the Δv received by the fragments at the breakup. Fig. 5 represents the data in terms of share of fragments in the same Δv range, whereas Fig. 1 can be useful to recall the distribution in terms of absolute numbers. One can observe how for $\Delta v < 400\,\mathrm{m/s}$ (where most fragments are) the ratio of impacts is almost independent on the Δv. It is also interesting to observe that around 13% of the fragments reach a condition of resonance with the Earth.

Finally, Fig. 6 shows the re-entry conditions for the objects in the fragment cloud. In this case, also a fragmentation on an orbit around L_2 is studied. The fragment cloud used for the simulation is the same of the case at L_1 to avoid that the comparison of the resulting distributions is affected by the random parameters of the NASA breakup model.

Both the distribution of the entry velocity and the one of the time interval between breakup and re-entry appear extremely similar for the two cases. In particular, the entry velocity is narrowly distributed around the valued of 11.05 km/s, in line, for example, with the results in [1].

For the other two quantities, fight path angle and latitude at the re-entry, the distributions appear different. For the latitude, for example, the two distributions have similar moments in absolute values, but opposite skewness.

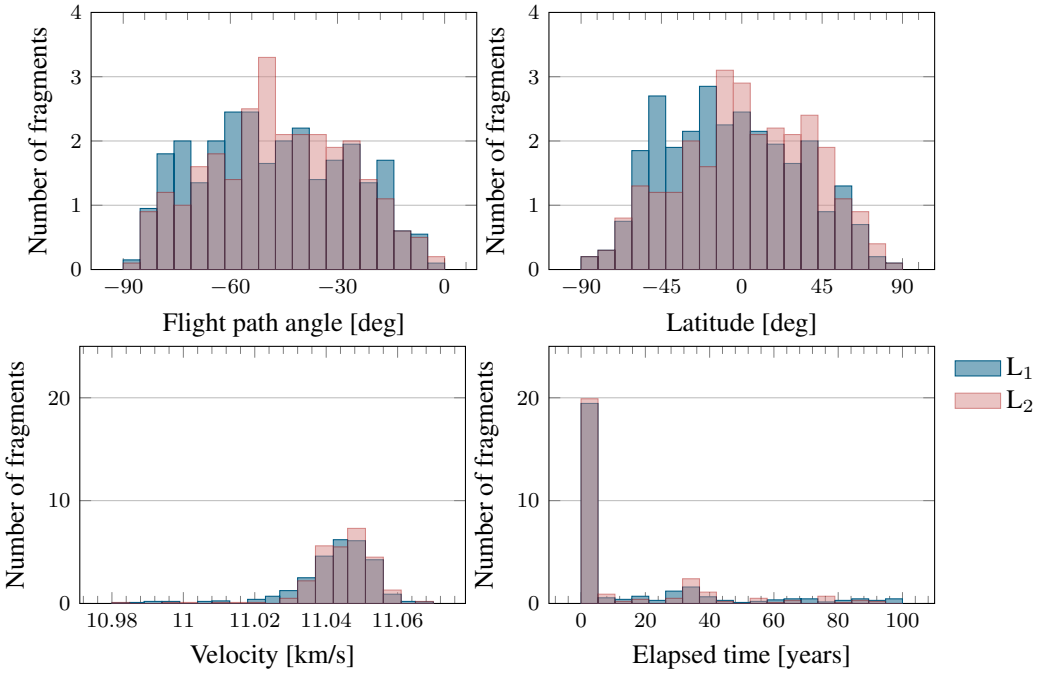

Figure 6. Distribution of the re-entry conditions for a fragmentation originating from orbits at L_1 and at L_2.

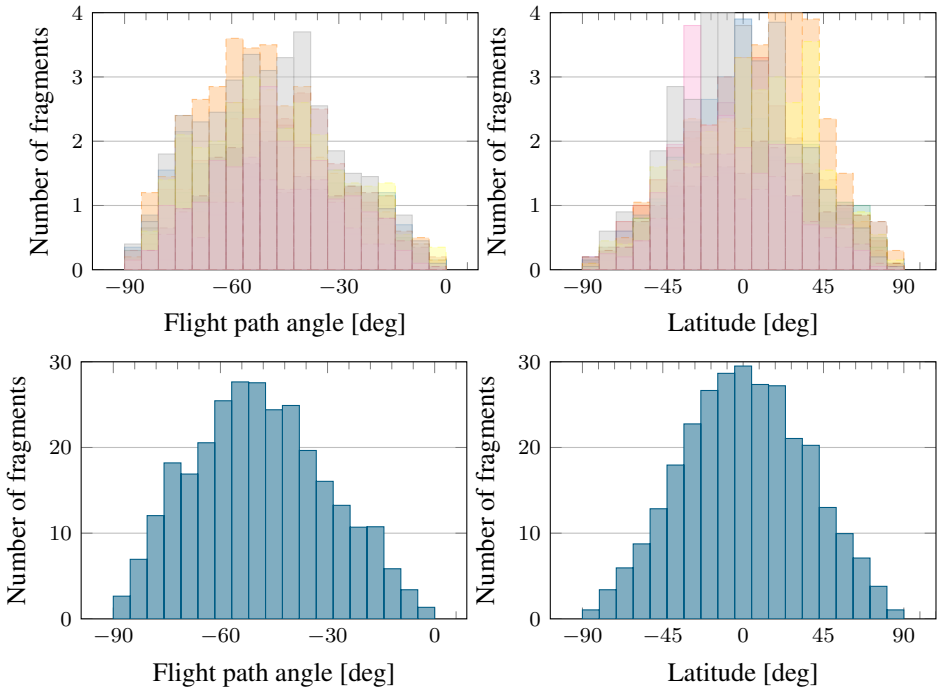

Figure 7. Distribution of flight path angle and latitude for fragmentations occurring on an orbit around L_2, at different epochs (top panels) and total (bottom panels).

To see how these distributions are affected by the fragmentation epoch, the same fragmentation was simulated in different epochs along the same LPO. Fig. 7 shows the result of these simulations for the case at L_2. The top panels represent the distributions for each epoch; the bottom panels the total distributions. It is clear how the location of the mean of the latitude distribution depends on the fragmentation epoch, whereas the distribution of the flight path angle appears less affected by this parameter. In both cases, the total distributions are not uniform.

Fig. 7 shows how one can build a distribution for the re-entry conditions without the need of introducing any *a priori* assumption. This may seem unnecessary complex for the case of a fragmentation at LPO considering that the potential threat posed by this kind of events is negligible with respect to collision and re-entry probability related to objects in LEO. On the other hand, the same analysis can be performed on the re-entry from LPO of intact spacecraft. In this case, an accurate representation of the entry conditions is important as it affects the resulting estimated casualty area. This can determine, for example, the necessity of performing a controlled re-entry and a consequent impact on the whole mission design. A first application in this field is discussed in the next section.

4. FAILURES AT THE LIBRATION POINTS

The second scenario studied in the current work is the one of the potential failure of a spacecraft on a LPO and the computation of the resulting re-entry probability. For this scenario, SNAPPshot generates a random failure time and the spacecraft state is obtained by interpolation from the nominal trajectory. SNAPPshot can automatically determine the required number of runs to verify a given requirement defined in terms of probability (e.g. the re-entry probability) and confidence level [8]. As a reference, to demonstrate a requirement of a probability below 1×10^{-4} with a confidence level of 99%, more than $50\,000$ runs are required. In this case, however, we cannot directly measure the casualty probability as this analysis is performed in post-processing with a dedicated tool such as DRAMA. To perform such an analysis, we would like to generate an appropriate number of re-entry trajectories to give statistical meaning to the results obtained with DRAMA.

In this work, the failure of a spacecraft on a LPO at L_2 is considered. As in the previous case, twelve different subscenarios were considered, each one corresponding to a launch in a different month and to around nine years of orbit evolution. Fig. 8 shows the evolution of the estimated probability of impact (solid line) together with the extremes of the 0.95 confidence level interval (dashed line) as a function of the number of runs. Each line represents one of the twelve scenarios and one is highlight for clarity. From the graph appears that at least 10 000-20 000 are required to obtain a stable estimation of the probability of impact.

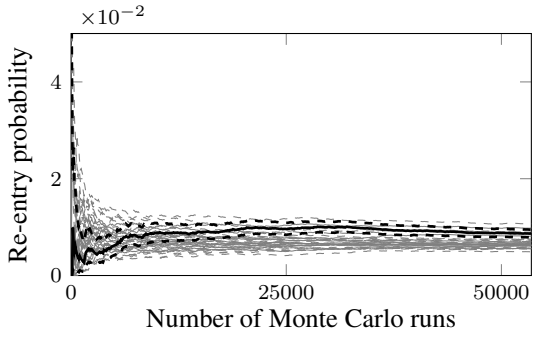

Figure 8. Estimated probability of impact (solid line) together with the extremes of the 0.95 confidence level interval (dashed line) as a function of the number of runs.

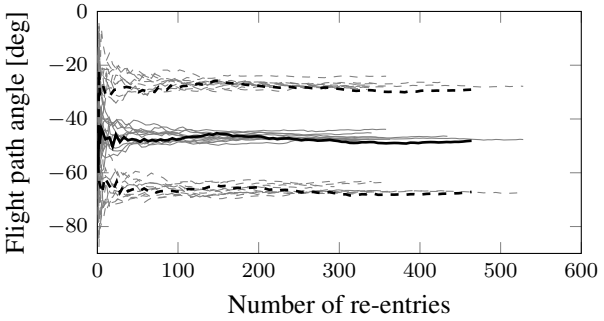

Figure 9. Mean (solid line) and mean ± standard deviation (dashed line) as a function of the number of re-entries.

A similar analysis was performed on the resulting distributions of flight path angle and latitude for each scenario. Fig. 9 shows the evolution of the mean and of the standard deviation of the flight path angle distribution as a function of the number of re-entries. In this case, the values seem to become stable when at least 200 re-entries are recorded. This value, combined with the estimated probability of impact, can be used to assess the minimum number of runs required to perform the analysis in the following. In this work, $50\,000$ runs per scenario are considered.

As for the case of fragmentations, flight path angle, latitude, entry velocity (Fig. 10) and elapsed time before re-entry are recorded. Whereas the distribution of the entry velocity is practically unchanged, the time of re-entry has now a peak at around 40 years from the moment of failure. For what concerns flight path angle and latitude, they appear to be highly correlated (Fig. 11) when the propagation is carried out including only the Sun, the Earth and the Moon[1]. In particular, the ellipses in Fig. 11 represent the unstable manifold intersecting with the Earth on the short term. This geometry vanishes once the effect of other planets is added to the propagation (Fig. 12).

[1] In this case the probability of impact with the Earth is also higher and equal to 6% compared to 1% when also the other planets are included in the propagation

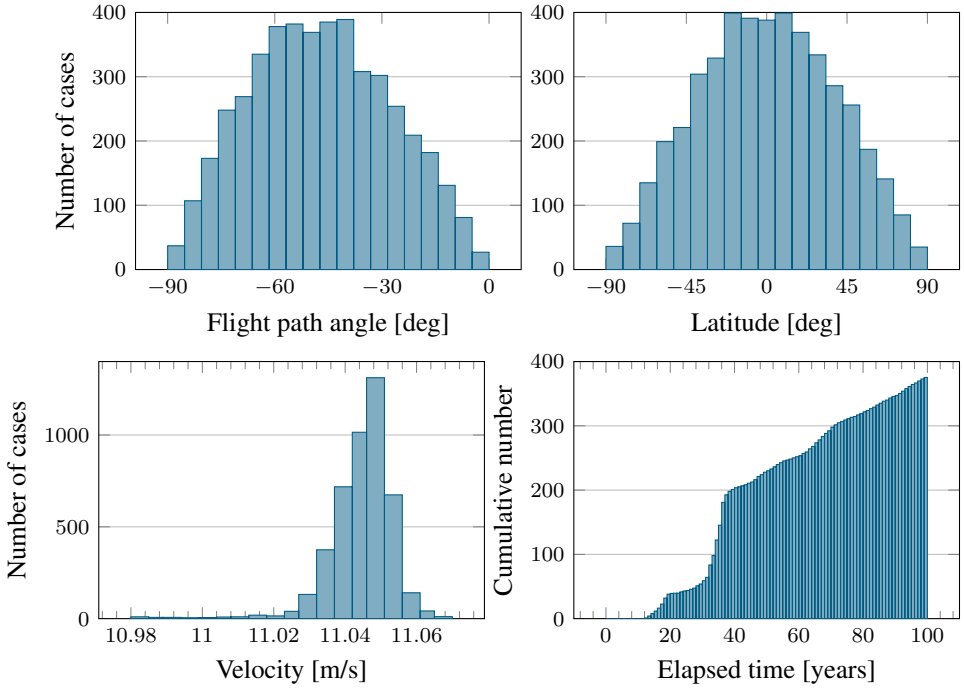

Figure 10. Distribution of the re-entry conditions considering all the twelve scenarios.

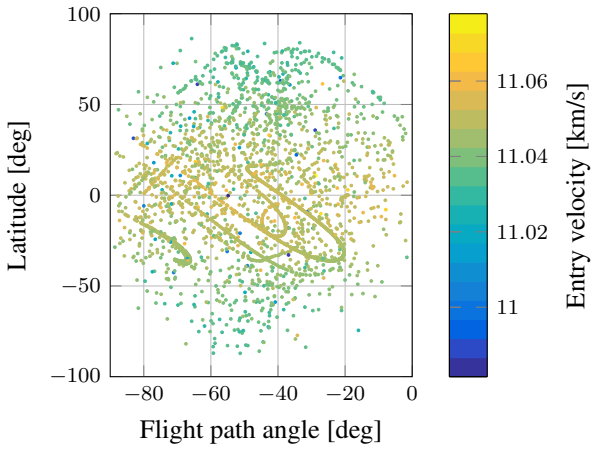

Figure 11. Distribution of the flight path angle and latitude of the re-entry points for one of the studied scenarios. Only the gravitational effect of Sun, Earth, and Moon is considered.

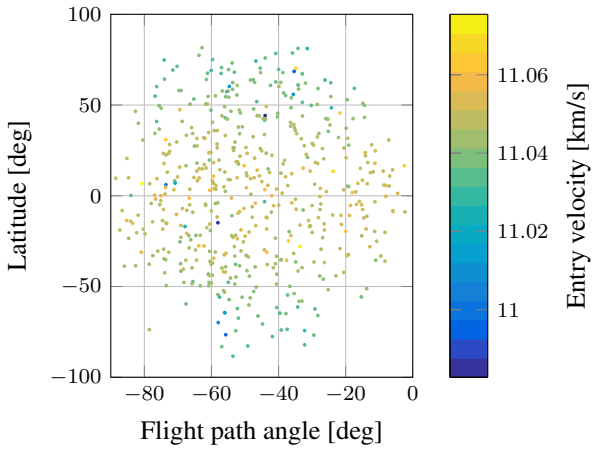

Figure 12. Distribution of the flight path angle and latitude of the re-entry points for one of the studied scenarios.

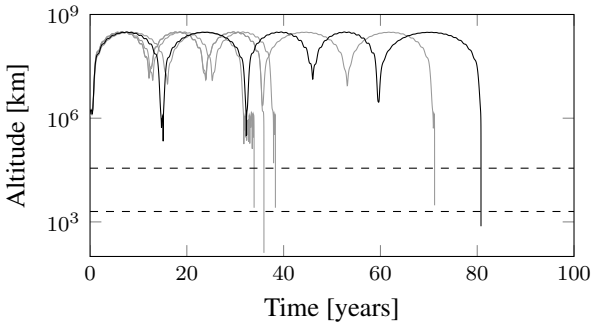

Figure 13. Evolution of five re-entry trajectories for the first scenario. The dashed lines refer to the GEO altitude and the upper boundary of LEO.

Similarly to the previous application, also in this case a further analysis of single trajectories is possible. Fig. 13 shows the evolution of five re-entry trajectories for the first scenario. The horizontal lines refer to the the upper boundary of LEO (2000 km) and to the GEO altitude. For trajectories with altitude close to the geostationary one an additional check is performed to verify if the spacecraft crosses the protected region around GEO. In this way, one can estimate also if any violation of the protected region occurs.

As mentioned in Section 2, the propagation performed with SNAPPshot is stopped at 120 km altitude. The final leg of the re-entry trajectories is analysed with the break-up prediction tool DRAMA/SARA [5], which models and simulates the spacecraft components as individual objects. A representative spacecraft model is selected for the analysis performed in this paper.

Each object trajectory is then independently propagated after it is separated from the parent spacecraft structure at a predefined break-up altitude. Typically, a standard altitude of about 78 km is selected. The value has been determined from re-entry observations of objects decaying from mostly circular orbits. Considering the properties of LPO re-entry trajectories, i.e. a larger re-entry velocity and steeper flight path angle, this altitude is not necessarily valid anymore [7].

In order to illustrate the impact of flight-path angle (β) and re-entry velocity, the re-entry of a simple cylindrical object with the mass of 5 tonnes has been simulated. Two scenarios are simulated: the first assumes a re-entry with an initial velocity of 7 km/s, corresponding to velocity of a typical circular decay, the second one models the LPO conditions with an initial velocity of 11 km/s. Figures 14 and 15 show the resulting loading profile (deceleration) and temperature increase of the respective cases. In case of the circular re-entry velocity, the deceleration appears more abruptly for steeper flight-path angles, i.e. it rapidly increases orders of magnitude. However, later during the decent it reaches approximately the same level as the circular $\beta = 0$ case. The temperature profile of the same case indicates that a steep re-entry angle leads

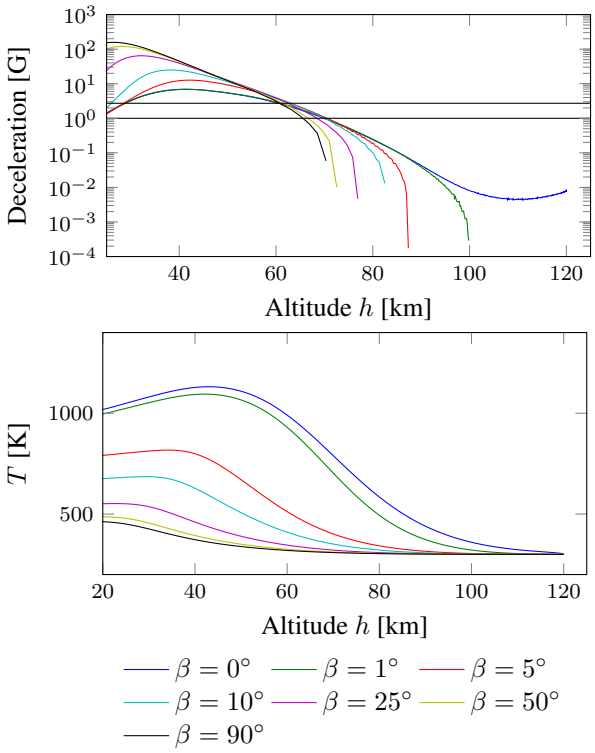

Figure 14. Temperature and deceleration profile for different flight-path angles β using a velocity of about 7 km/s at the initial state (circular decay in case of $\beta = 0$).

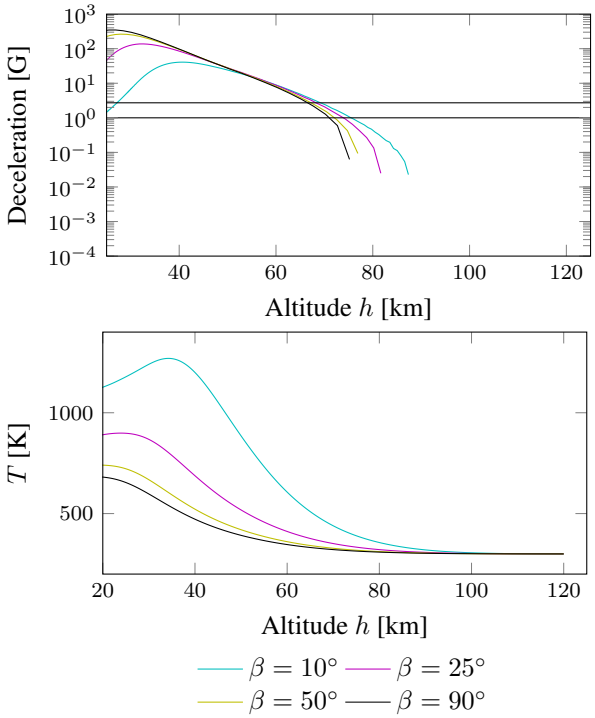

Figure 15. Temperature and deceleration profile for different flight-path angles β using a velocity of about 11 km/s at the initial state.

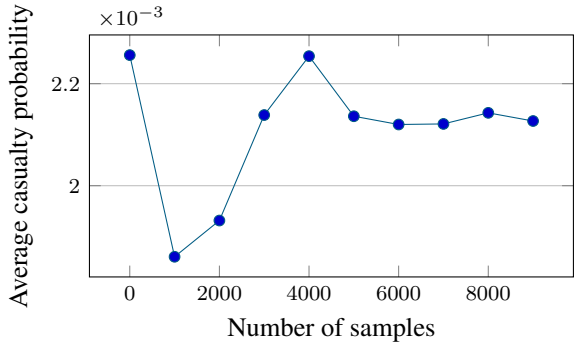

Figure 16. Evolution of the average casualty probability as a function of the number of generated samples.

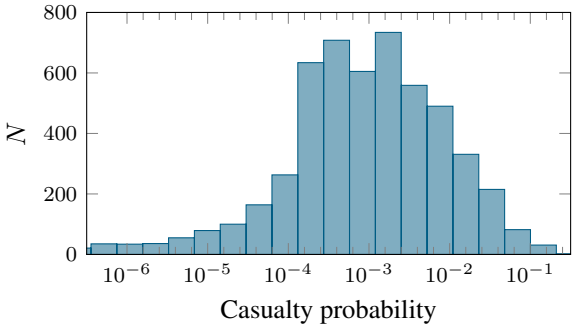

Figure 17. Distribution of the casualty probability.

to a smaller peak temperature. In case of the LPO scenario (11 km/s initial velocity), one can observe the same relationship between loading and peak temperature depending on flight-path angle. A steeper flight path angle leads to a faster altitude decrease, giving the objects less time to heat up. However, the large impact velocity increases the temperature and loading when entering the atmosphere, which could lead to a break-up at a higher altitude. The coupling of the two effects must be studied more in detail. For the analysis performed here, a 60 km break-up altitude is selected. It is important to note that the simulations above only consider convective heating as transfer mechanism, and omit the contributions from radiative heat transfer which can be significant for these high velocity entry conditions. The low break-up altitude at an initial low temperature with convective heating only is thus a conservative approach to study the impact.

The interface between SNAPPshot and DRAMA is set after the Monte Carlo simulation and the generation of the re-entry conditions at 120 km. For the current application, the distribution of re-entry trajectories for all the launch epochs (Fig. 10), which counts a total of 4566 elements, is re-sampled in around 10 000 samples to obtain a confident estimate of the casualty risk (Fig. 16). Each sample is used to start a break-up and re-entry simulation. To obtain the distribution of the casualty probability shown in Fig. 17, the distribution of the resulting re-entry locations for the re-sampled distribution is shown in Fig. 18. Out of 10 000 samples, 7 370 drop down in the ocean and consequently have a casualty risk of 0. The risk distribution of the remaining samples is what is shown in Fig. 17. The average risk, taking all samples into account, accumulates to 2.127×10^{-3}. It was observed that this value is around twice the average casualty probability obtained assuming a break-up altitude of 78 km. This casualty risk must be scaled with the re-entry probability in order to derive the overall risk estimate for the mission.

5. CONCLUSIONS

This paper analysed the re-entry conditions for objects in orbit at the Sun-Earth libration points using the tool SNAPPshot for the generation of the trajectory and DRAMA/SARA for the break-up prediction.

First, the case of a fragmentation was studied considering the resulting trajectories for the produced fragments. In particular, the probability of impact and the distribution of the minimum distance with respect to the Earth were analysed, finding a good level of consistency with a previous study on the same topic. In addition, the resulting distribution of flight path angle, latitude and entry velocity were derived, both for fragmentations at L_1 and at L_2, finding a similar behaviour. The effect of the fragmentation epoch was also analysed showing how it affects the mentioned distributions.

The second application presented in the paper is the study of re-entries from the libration points due to on-orbit failure of a spacecraft. The first task for this application was to estimate the required number of Monte Carlo runs to obtain a stable estimation of the re-entry probability and of the parameters of the distributions of the re-entry conditions. An example case was studied considering twelve possible launch dates and running for each scenario 50 000 Monte Carlo simulations. The resulting distributions of re-entry latitude and flight path angle can be considered not correlated and so they were re-sampled to generate a total of 10 000 re-entry conditions. Each condition was analysed in DRAMA/SARA, assuming a breakup altitude equal to 60 km. The resulting distribution of the casualty probability is then obtained and it can be used to assess the compliance of the mission with Space Debris Mitigation guidelines. In addition, SNAPPshot can also be used to identify crossings with the protected regions, so that the proposed methodology can be employed to have a general evaluation of the performance of mitigation actions for missions at the libration points.

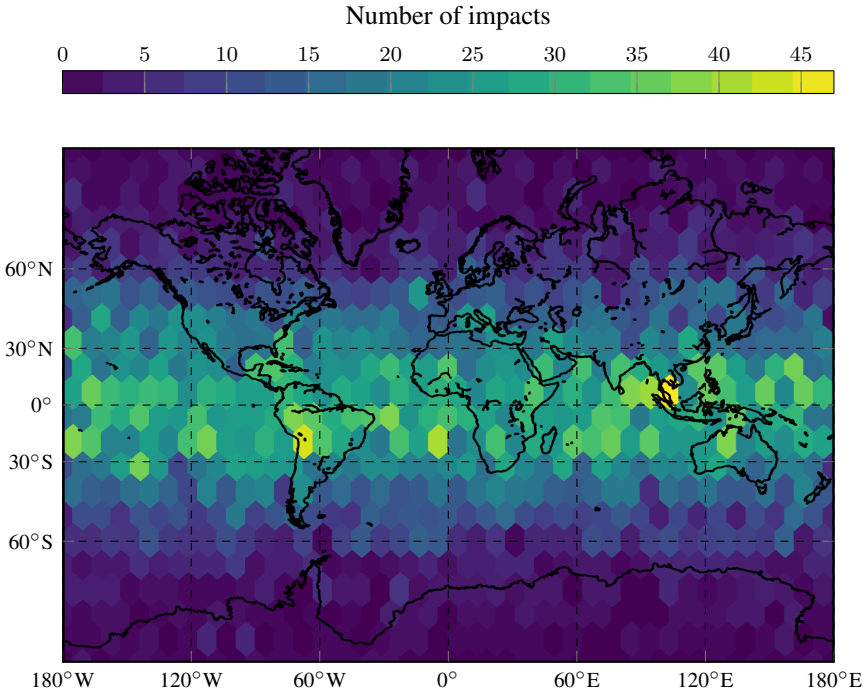

Figure 18. Distribution of entry locations.

ACKNOWLEDGMENTS

Francesca Letizia thanks ESA Space Debris Office and Mission Analysis Section for the support received during her visiting period in ESOC where part of this work was developed. The authors acknowledge the use of the IRIDIS High Performance Computing Facility, and associated support services at the University of Southampton, in the completion of this work.

REFERENCES

1. Alessi E. M. (2015), The reentry to earth as a valuable option at the end-of-life of libration point orbit missions, *Advances in Space Research*, 55(12): 2914–2930.
2. Braun V., Gelhaus J., Kebschull C., Sánchez-Ortiz N., Oliveira J., Domínguez R., Wiedemann C., Krag H., and Vörsmann P. (2014), DRAMA 2.0 - ESA's space debris risk assessment and mitigation analysis tool suite, In *65th International Astronautical Congress*. International Astronautical Federation, IAC-14-A.6.4.4.
3. Colombo C., Alessi E. M., van der Weg W., Soldini S., Letizia F., Vetrisano M., Vasile M., Rossi A., and Landgraf M. (2015), End-of-life disposal concepts for libration point orbit and highly elliptical orbit missions, *Acta Astronautica*, 110:298–312.
4. Johnson N. L. and Krisko P. H. (2001), NASA's new breakup model of EVOLVE 4.0, *Advances in Space Research*, 28(9):1377–1384.
5. Klinkrad H., Fritsche B., and Lips T. (2004), A standardized method for re-entry risk evaluation, In *55th International Astronautical Congress*. International Astronautical Federation.
6. Landgraf M. and Jehn R. (2001), Space debris hazards from explosions in the collinear sun-earth lagrange points, In *Third European Conference on Space Debris*.
7. Lemmens S., Merz K., Bonvoisin B., Lhle S., and Simon H. (2017), Planned yet uncontrolled re-entries of the cluster-ii spacecfraft, In *Seventh European Conference on Space Debris*.
8. Letizia F., Colombo C., Van den Eynde J., Armellin R., and Jehn R. (2016), SNAPPSHOT: Suite for the numerical analysis of planetary protection, In *6th International Conference on Astrodynamics Tools and Techniques*.
9. Letizia F., Colombo C., Van den Eynde J., and Jehn R. (2016), B-plane visualisation tool for uncertainty evaluation, In *26th AAS/AIAA Space Flight Mechanics Meeting*.
10. Olikara Z. P., Gómez G., and Masdemont J. J. (2015), Dynamic mechanisms for spacecraft disposal from sun–earth libration points, *Journal of Guidance, Control, and Dynamics*, 38(10):1976–1989.